GEOLOGICA CARPATHICA, 48, 5, BRATISLAVA, OCTOBER 1997
287–302

PRESSURE-TEMPERATURE CONDITIONS OF HIGH-GRADE METAMORPHISM AND MIGMATITIZATION IN THE MALÁ FATRA CRYSTALLINE COMPLEX, THE WESTERN CARPATHIANS

MARIAN JANÁK* and BRANISLAV LUPTÁK

Department of Mineralogy and Petrology, Faculty of Sciences, Comenius University, Mlynská dolina, 842 15 Bratislava, Slovak Republic

(Manuscript received October 9, 1996; accepted in revised form June 24, 1997)

Abstract: Pressure-temperature conditions of metamorphism and migmatitization were investigated in the Malá Fatra crystalline complex, representing one of the deepest segments of the Variscan basement in the Western Carpathians. Field observations together with structural data document close relationships between migmatitization and deformation. The penetrative, syn- to post-metamorphic Variscan deformation with generally top-to-the south-southeast sense of shearing has been documented. Thermobarometric data obtained by conventional and internally consistent (TWEEQU) methods indicate the attainment of ca. 700–750 °C and 6 kbar in metapelitic migmatites and 700–750 °C and 8–10 kbar in garnet-clinopyroxene amphibolites. Migmatitization took place by partial melting during decompression, producing granitic leucosome in metapelites and tonalitic-trondhjemitic one in the metabasites. Initial high-pressure stage and a "clock-wise" P-T path is inferred from a) kyanite-sillimanite transformation in metapelites and b) kelyphitic and symplectitic textures in garnet-clinopyroxene metabasites, indicating the breakdown of eclogites reequilibrated at upper-amphibolite to granulite facies conditions. The proposed metamorphic evolution is consistent with considerable crustal thickening and extension of the West-Carpathian crystalline basement during the Variscan orogeny.

Key words: Western Carpathians, Malá Fatra, Variscan orogeny, high-grade metamorphism, thermobarometry, deformation, migmatites.

Introduction

The Malá Fatra crystalline complex represents one of the deepest segments of the pre-Mesozoic basement exposed in the Central Western Carpathians. One of the most striking features of this crystalline complex is widespread migmatitization, observed in paragneisses as well as amphibolites (e.g. Hovorka 1969, 1974). The metamorphic conditions in the Malá Fatra Mts. have been estimated by several authors (Perchuk et al. 1984; Korikovsky et al. 1987; Krist et al. 1992; Hovorka & Méres 1991; Hovorka et al. 1993), who suggested the attainment of amphibolite facies. However, relict assemblages indicating a higher-pressure (eclogite facies) metamorphism in metabasites have also been reported (Hovorka et al. 1992).

In this study, we present new thermobarometric data from both migmatitic metapelites and metabasites which suggest their generation by partial melting at the upper amphibolite-granulite facies transition, most probably during decompression from higher-pressure, eclogite facies conditions. The aim of this paper is also to emphasize the role of ductile deformation in melt segregation during the Variscan evolution of the Malá Fatra crystalline complex.

Geological setting

The Malá Fatra Mts. represent a typical core complex located in the furthest northwestern protrusion of the Tatric Unit in the Central Western Carpathians. The crystalline basement consists of two partial segments — the Veľká Lúka Massif in the west and the Kriváň Massif in the east, separated by a NNW–SSE trending Alpine fault. The investigated area is the southeastern part of the Veľká Lúka Massif (Fig. 1) where metamorphic rocks are abundant in contrast to the northern part — the Kriváň Massif, which is mainly composed of granitoids (Ivanov & Kamenický 1957; Benko 1996; Broska et al. 1997).

Metamorphic rocks in the Veľká Lúka Massif represent several lithological types of sedimentary as well as igneous pre-metamorphic origin, which have been affected by high-grade metamorphism and migmatitization (Fig. 1). Metapelites are represented by biotite, garnet and sillimanite paragneisses exhibiting migmatitization. Orthogneisses with characteristic augen texture and mylonitic fabric are thought to represent former granitoids, and/or acid volcanic rocks (Kamenický & Macek 1984). Metabasites are represented by several types of amphibolites: fine- to coarse-grained amphibolites, massive garnet and garnet-clinopyroxene amphibolites, banded and migmatitic amphibolites to amphibole gneisses. Rare metaultramafic rocks have been described as amphibole peridotites (Ivanov & Kamenický 1957; Hovorka et al. 1985). Sporadic calc-silicates have also been reported (Korikovsky et al. 1987).

The granitoids in the Veľká Lúka Massif correspond to tonalites and hybrid tonalites (Kamenický et al. 1987). They are crosscut by lamprophyric dykes (Ivanov & Kamenický 1957; Hovorka 1967). The U-Pb zircon age of tonalite from the quarry Dubná Skala is 353 Ma, according to Scherbak et al. (1990).

The structural relations between the metamorphic rocks and granitoids can be best studied in the profile across Mlynský

*Present address: Geological Institute, Slovak Academy of Sciences, Dúbravská 9, 842 26 Bratislava, Slovak Republic

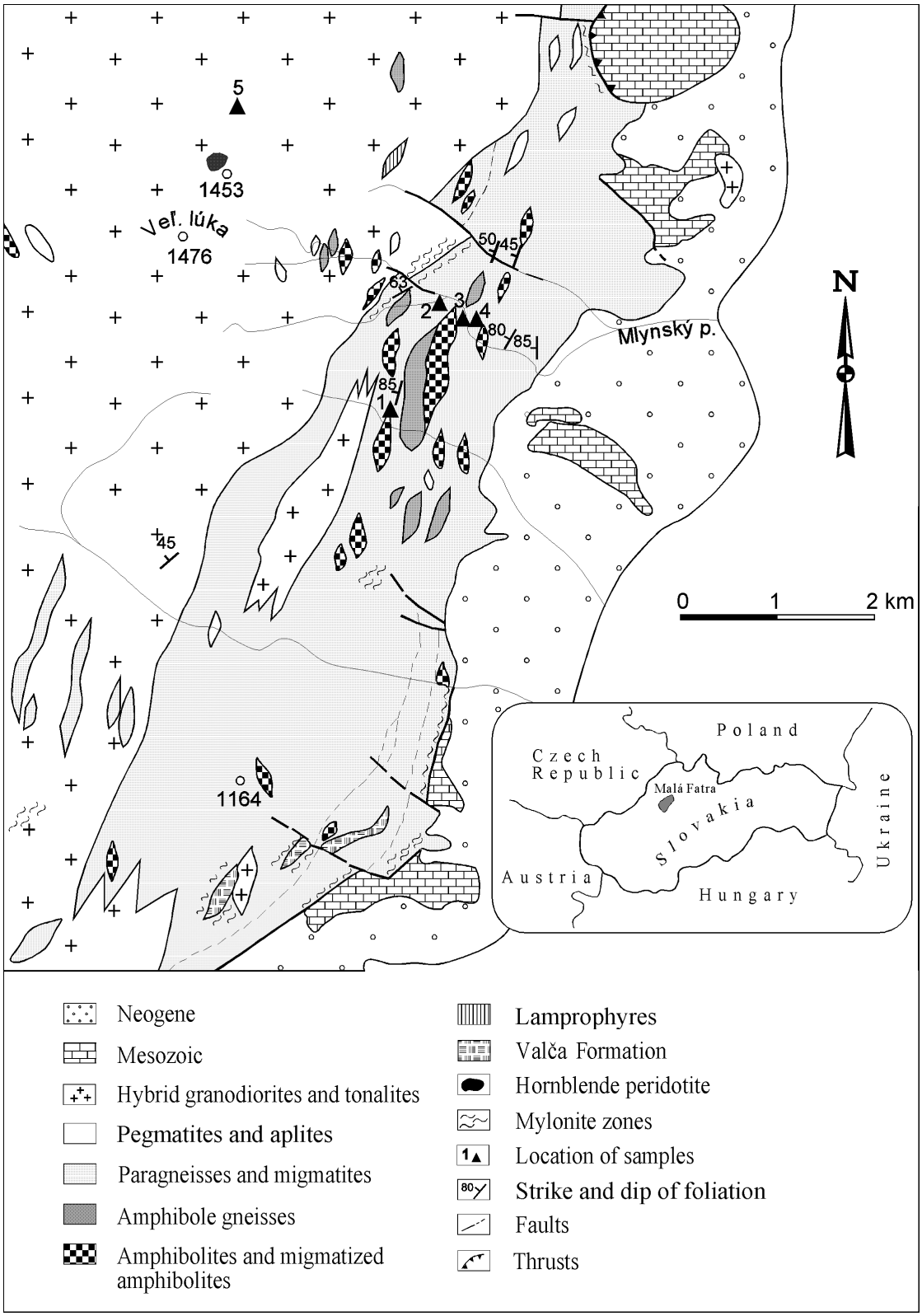

Fig. 1. Schematic geological map of the southern part of the Malá Fatra — Veľká Lúka Massif.

Potok — Veľká Lúka 1470 m e.p. (Fig. 2). Structurally upwards, the metamorphic rocks show increasing migmatitization and leucosome vs. paleosome proportions. Thus, the migmatites pass gradually into the hybrid tonalites in the uppermost levels of the entire sequence.

The metamorphic foliation moderately to steeply dips to the NW (Figs. 1, 2). Mineral lineation, as defined by elongation of biotite, sillimanite and amphibole, varies between NW-SE and N-S direction. The metamorphic rocks dip beneath granitoids and there is no intrusive penetration of

metamorphic rocks by granitoids from beneath. Numerous ductile shear zones indicate high temperature conditions of deformation; brittle deformation is characteristic of younger faults crosscutting metamorphic foliation. These can be temporally connected with Alpine tectonic processes. However, most of the ductile mesoscopic structures and kinematic indicators, e.g. asymmetric feldspar porphyroclasts indicate that the (sense) direction of major tectonic transport was top-to-the SSE-SE. This is attributed to Variscan deformation (Lupták 1996).

Petrography and mineral chemistry

The chemical compositions of selected minerals were determined using JEOL 733 electron microprobe at Geological Institute of Dionýz Štúr (Geological Survey of the Slovak Republic) in Bratislava. A point beam at operating conditions of 10 nA and 15 kV was used. The data were reduced by the ZAF correction method. Mineral abbreviations in this paper are given according to Kretz (1983).

Garnet-sillimanite gneisses and metapelitic migmatites

The migmatitization in metapelitic gneisses is shown by inhomogeneous texture, with characteristic segregations into the leucosome, melanosome and/or mesosome (nomenclature according to Ashworth 1985). Leucosome is coarse grained, sometimes pegmatoid-like, composed of variable contents of plagioclase, quartz and K-feldspar, thus corresponding to granite-granodiorite composition. Mesosome is fine- to medium-grained. The most common mineral assemblages include: garnet + sillimanite + biotite + quartz + plagioclase ± K-feldspar ± muscovite with ilmenite and minor amount of rutile as Fe-Ti oxides. Melanosome consists of accumulations and selvadges of biotite.

The texture is mostly stromatitic, with alternating leucocratic and melanocratic layers. The lineation is defined by the alignment of biotite and/or biotite + sillimanite aggregates, as well as long dimensions of quartz ribbons. Asymmetric porphyroclasts of feldspars and shear bands which deform the foliation indicate a shear component of the deformation. The leucocratic material is often located in the shears, boudin necks and dilation fractures, indicating that the melt was focused into a tectonically weakened shear zones and veins forming an anastomosing network (Fig. 3). With increasing portions of leucosome, the texture becomes more homogeneous; thus, the migmatites (diatexites) are passing gradually into the hybrid granitoids.

Garnet forms porphyroblasts of varying size, mostly less than 1–2 mm in diameter, but in some cases they reach up to 10 mm. The majority of garnets are idiomorphic (Fig. 4a), indicating equilibrium with the matrix, whereas some garnets show resorption in the rims due to rection with the biotite. In-

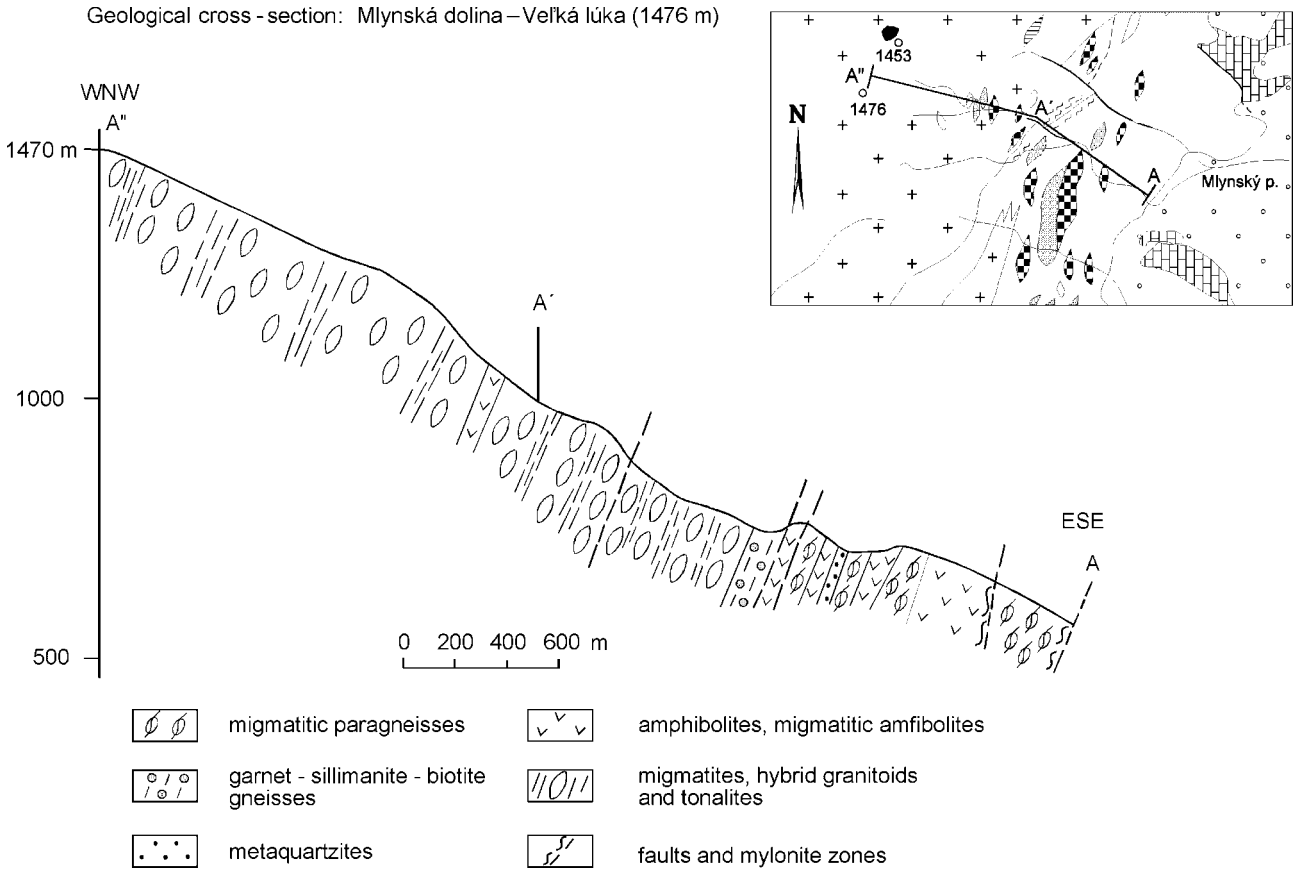

Fig. 2. Geological cross-section of the Veľká Lúka Massif in the southern part of the Malá Fatra.

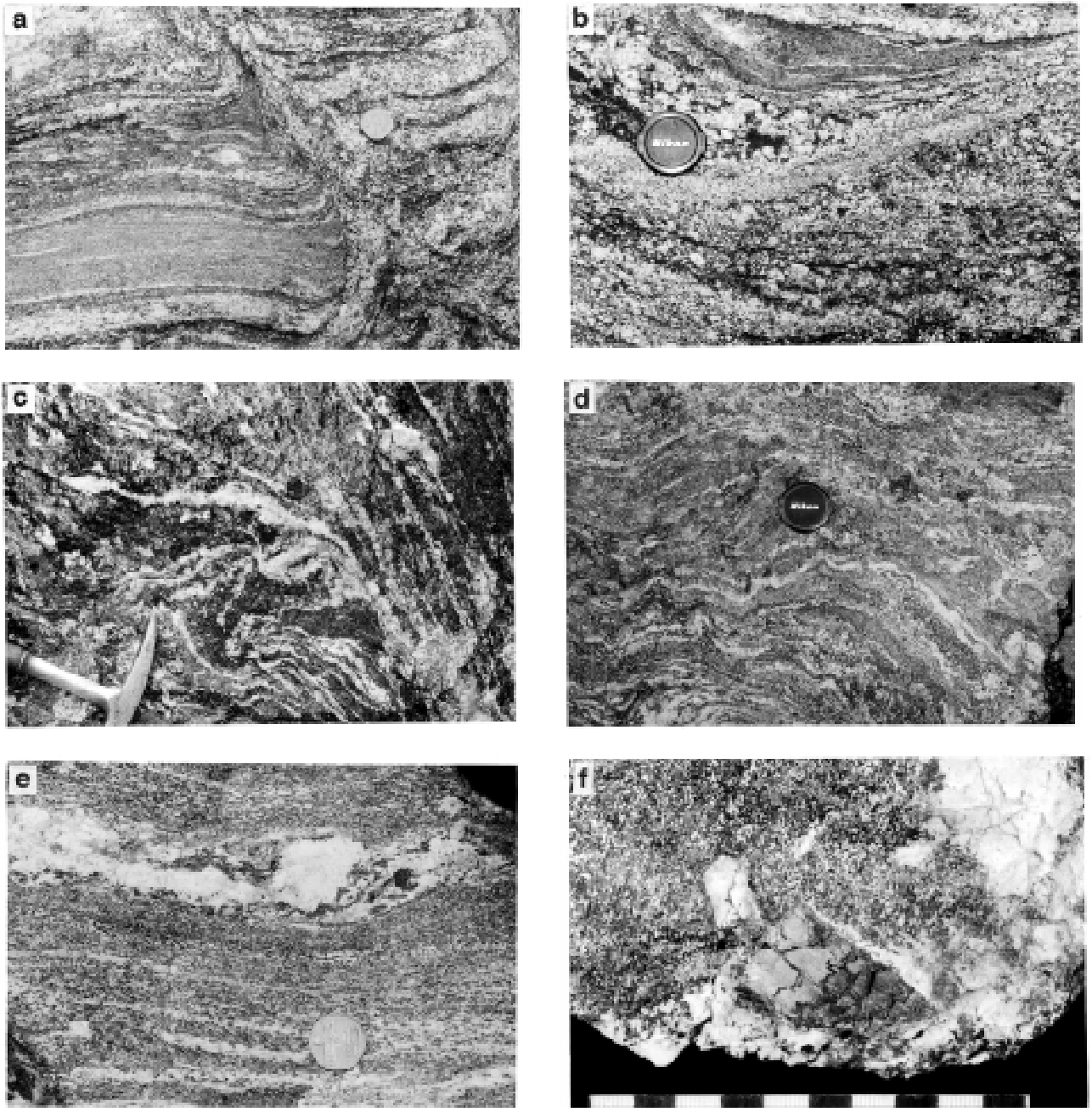

Fig. 3. Migmatite textures in the Malá Fatra crystalline complex. **a** — Melt segregetion into the shear bands in the metapelitic migmatite, **b** — coarse-grained metapelitic diatexite, **c** — tonalitic-trondhjemitic veins and segregations in amphibolite, **d** — thin leucosome, layer-parallel oriented and folded in the amphibolite, **e** — segregation of coarse-grained plagioclase-quartz-amphibole leucosome in amphibolite, **f** — "recrystallized" amphibole in tonalitic-trondhjemitic leucosome at the contact with fine-grained amphibolite.

clusions of biotite, plagioclase and quartz are sometimes present in the garnet cores. Garnet composition (Table 1) corresponds to a mixture of almandine (65–75 %) and pyrope (15–30 %) component with low grossular (3–4 %) and spessartine (2–5 %) contents. The majority of the garnets show no substantial changes in composition, except for the outermost part of grains where almandine and the Fe/(Fe+Mg) ratio increases and the pyrope decreases with respect to the core (Fig. 5). Spessartine contents across the grain are constant, or increase in the rims.

Homogeneous compositions in the garnet cores are interpreted as the result of intragranular diffusion at high temperature (Yardley 1977; Woodsworth 1977), combined with intergranular diffusion (Spear 1991) modifying the garnet rim due to retrograde exchange reaction between the garnet and biotite (increasing Fe/Fe+Mg in the garnet). Preferential fractionation of Mn into the garnet is thought to be the consequence of the retrograde, garnet-consuming net-transfer reaction garnet + K-feldspar + H_2O = biotite + sillimanite + quartz. This can be deduced from the biotite-sillimanite inter-

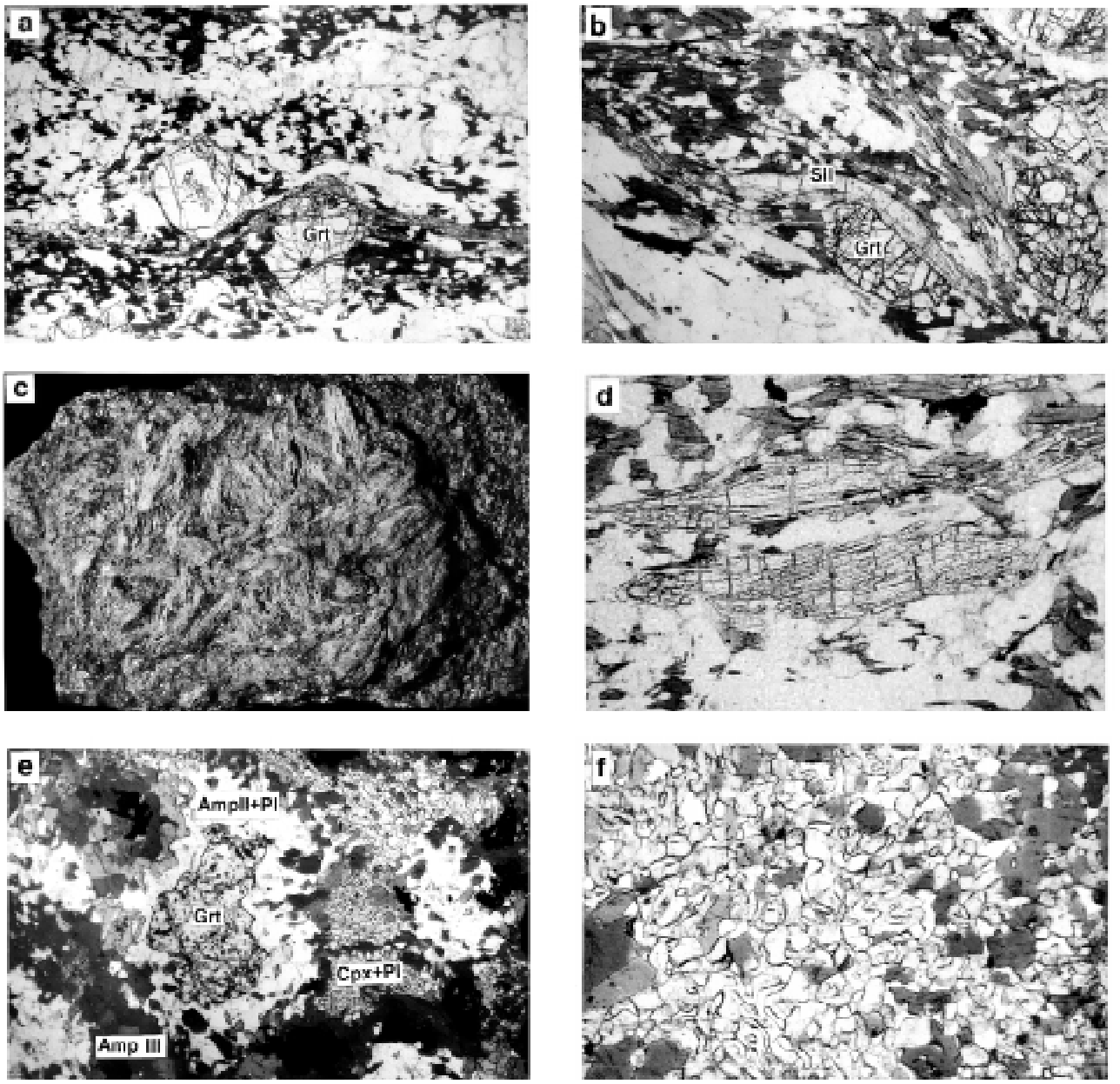

Fig. 4. Photomicrographs of: **a** — biotite, sillimanite and garnet porphyroblasts in the mesosome of metapelitic migmatite exhibiting mylonitic SC fabric, width of view is 10 mm; **b** — prismatic sillimanite wrapped around the garnet in metapelitic migmatite, width of view is 10 mm; **c** — randomly oriented aggregates of sillimanite probably pseudomorphing kyanite in metapelite; **d** — photomicrograph of thick sillimanite, indicating the transformation of former kyanite to sillimanite in metapelite, width of view 8 mm; **e** — characteristic breakdown textures in garnet-clinopyroxene amphibolite with kelyphitic rim of amphibole and plagioclase (Amp II+Pl) around garnet (Grt) and symplectites of clinopyroxene with plagioclase (Cpx+Pl) replaced by amphibole (Amp III). Width of view is 15 mm; **f** — symplectite of clinopyroxene+plagioclase invaded by amphibole (dark-grey) indicating the breakdown of omphacite in garnet-clinopyroxene amphibolite. Width of view is 2 mm.

growths around the resorbed subhedral garnets in the presence of K-feldspar in the matrix.

Sillimanite occurs both in the form of prismatic crystals and fibrolite (Fig. 4a,b). Large needles up to 1cm thick and 2–3 cm long form aggregates and knots (Fig. 4c), which indicate the presence of former kyanite transformed into sillimanite. However, only sillimanite has been detected by X-ray diffraction. Prismatic sillimanite forms individual crystals or is intergrown with biotite in the matrix. Large sillimanite crystals are concordant with foliation and exhibit folding and bending, being often wrapped around the garnet and plagioclase porphyroclasts in the deformed matrix (Fig. 4a,b). Some of the sillimanite needles are disrupted by minor cracks, indicating the changing ductile-brittle and compressional-tensional regime during deformation. Consequently, the alignment of sillimanite needles defines a syn- to post-crystalline deformation and transport during Variscan exhumation.

Feldspars occur mostly in the matrix where they are mostly segregated together with quartz, forming the leucosome. Plagioclase inclusions (An_{50}) are only sporadically present in the

Table 1: Chemical compositions of garnet.

garnet-sillimanite gneisses					garnet-clinopyroxene amphibolite						
	MF14/94		**MF13**		**MF 16**						
	grt 1	**grt 11**	**grt 2**	**grt 4**	**grt 1**	**grt 2**	**grt 3**	**grt 4**	**grt 14**	**grt 17**	**grt 20**
	core	rim	core	rim	rim	core		rim			rim
SiO_2	37.65	37.26	37.61	37.10	37.30	37.85	37.97	38.01	36.96	38.19	37.83
Al_2O_3	22.69	21.78	22.00	22.07	22.07	21.31	20.71	20.95	21.45	21.06	21.04
TiO_2	0.00	0.00	0.00	0.03	0.03	0.07	0.07	0.03	0.00	0.07	0.05
MgO	7.73	5.10	5.03	3.54	3.10	2.49	2.68	3.17	2.67	2.42	3.24
FeO	29.86	32.86	27.73	26.32	27.51	27.61	27.57	26.44	29.04	27.63	27.34
MnO	0.83	0.93	6.98	10.16	1.75	2.26	1.02	1.74	1.69	1.17	1.31
CaO	1.29	1.20	2.89	2.38	8.22	8.60	8.89	8.84	8.10	8.87	9.20
Σ	100.05	99.13	102.24	101.60	99.98	100.19	98.91	99.18	99.91	99.41	100.01
Recalculated on the basis of 12 oxygens											
Si	2.934	2.977	2.934	2.935	2.953	3.000	3.036	3.023	2.953	3.037	2.995
Al	2.084	2.051	2.023	2.058	2.059	1.991	1.951	1.964	2.020	1.974	1.963
Ti	0.000	0.000	0.000	0.002	0.002	0.004	0.004	0.002	0.000	0.004	0.003
Mg	0.898	0.608	0.585	0.418	0.366	0.294	0.319	0.376	0.318	0.287	0.382
Fe^{2+}	1.946	2.196	1.809	1.741	1.821	1.830	1.843	1.759	1.940	1.837	1.810
Mn	0.055	0.063	0.461	0.681	0.117	0.152	0.069	0.117	0.114	0.079	0.088
Ca	0.108	0.103	0.242	0.202	0.697	0.730	0.762	0.753	0.693	0.756	0.780
$Fe^{2+}/Fe^{2+}+Mg$	0.684	0.783	0.756	0.806	0.833	0.862	0.852	0.824	0.859	0.865	0.826
Prp	0.299	0.204	0.189	0.137	0.122	0.098	0.107	0.125	0.104	0.097	0.125
Alm	0.647	0.740	0.584	0.572	0.607	0.609	0.616	0.585	0.633	0.621	0.591
Sps	0.018	0.021	0.149	0.224	0.039	0.051	0.023	0.039	0.037	0.027	0.029
Grs	0.036	0.035	0.078	0.066	0.232	0.243	0.254	0.251	0.226	0.255	0.255

garnet cores. The compositions in the matrix correspond to oligoclase-andesine (Table 2). K-feldspar is restricted mostly to the segregated leucosomes. Rarely, it also occurs in the interstices between plagioclase and quartz in the muscovite-free mesosome, suggesting the overstepping of muscovite + quartz equilibrium in favour of K-feldspar stability during the initial stage of melting, e.g. the dehydration-melting reaction muscovite + plagioclase + quartz = K-feldspar + sillimanite + melt.

Biotite forms lath-shaped porphyroblasts, which commonly define the metamorphic foliation000000. The orientation of biotites indicates a simple shear regime with top-to-the east and southeast sense of transport during Variscan syn- to post-metamorphic deformation. Small biotites form inclusions in the cores of garnets.

The composition of biotites is shown in the Table 3. The nearly constant composition of the matrix biotites indicates that they were equilibrated at the same P-T conditions. Only a minor part of the biotite has been affected by chloritization during retrograde processes.

Muscovite forms large individual porphyroblasts, oriented in the planes of metamorphic foliation together with biotite, or across the foliation. In samples where K-feldspar is absent, muscovite may be considered as a stable phase during peak metamorphic conditions, i.e. below the stability of K-feldspar. On the other hand, in some samples muscovite is present together with K-feldspar. Such muscovite may be retrograde with respect to peak metamorphic conditions, as indicated by thermobarometry discussed below.

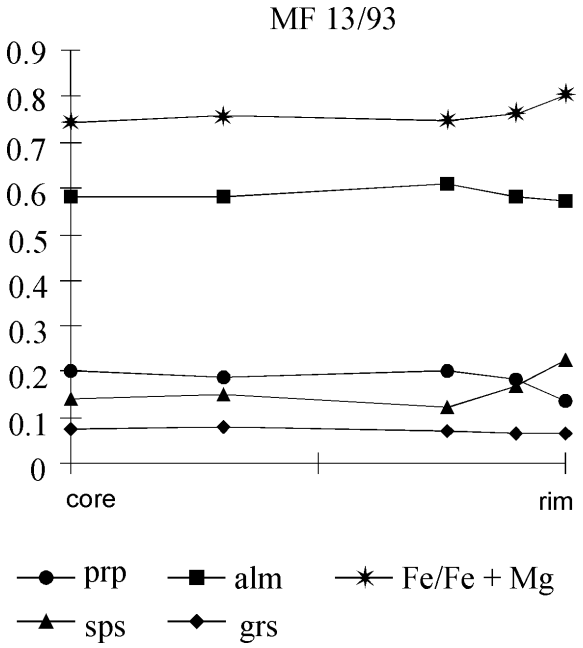

Fig. 5. Compositinal profile across garnet in the sample MF 13/93.

Garnet-clinopyroxene amphibolites and mafic migmatites

Amphibolites in the Malá Fatra show strong migmatitization on a centimetre to decimetre scale (Fig. 3). The texture is

Table 2: Chemical compositions of feldspars.

garnet-sillimanite gneisses					garnet-clinopyroxene amphibolite				
MF14/95			**MF13**		**MF 16**				
	plg 8	**Kfs**	**plg 1**	**plg 8**	**plg 18**	**plg 22**	**plg 23**	**plg 26**	**plg 38**
	next to grt	matrix	in grt	matrix	next to grt		in symplectites		
SiO_2	60.01	67.09	55.40	55.98	59.50	59.88	59.54	60.53	60.12
Al_2O_3	25.29	18.54	29.25	28.87	25.19	25.76	24.71	25.13	25.27
MgO	0.00	0.01	0.01	0.00	0.00	0.00	0.00	0.00	0.00
FeO	0.03	0.00	0.27	0.03	0.00	0.03	0.13	0.08	0.05
MnO	0.00	0.03	0.04	0.03	0.03	0.00	0.00	0.00	0.05
CaO	5.62	0.00	10.80	9.46	7.77	7.35	7.36	7.04	6.89
Na_2O	7.79	0.57	5.67	6.10	6.84	7.34	7.67	7.69	7.32
K_2O	0.10	15.56	0.10	0.04	0.16	0.27	0.16	0.16	0.19
Σ	98.83	101.80	101.55	100.51	99.49	100.63	99.57	100.63	99.89
Recalculated on the basis of 8 oxygens									
Si	2.691	3.024	2.463	2.500	2.665	2.654	2.672	2.681	2.678
Al	1.337	0.985	1.533	1.520	1.330	1.346	1.307	1.312	1.327
Mg	0.000	0.002	0.001	0.000	0.000	0.000	0.000	0.000	0.000
Fe^{2+}	0.001	0.000	0.010	0.001	0.000	0.001	0.005	0.003	0.002
Mn	0.000	0.001	0.002	0.001	0.001	0.000	0.000	0.000	0.002
Ca	0.270	0.001	0.515	0.453	0.373	0.349	0.354	0.334	0.329
Na	0.677	0.050	0.489	0.528	0.594	0.631	0.667	0.660	0.632
K	0.006	0.895	0.006	0.002	0.009	0.015	0.009	0.009	0.011
XAn	0.283	-	0.510	0.460	0.382	0.351	0.344	0.333	0.338
XAb	0.710	-	0.480	0.540	0.609	0.634	0.648	0.658	0.650
XOr	0.006	-	0.010	0.000	0.009	0.015	0.009	0.009	0.011

inhomogeneous, exhibiting layering and segregations into leucosome and more mafic mesosome. Melanosome is represented by amphibole-rich segregations, sometimes present at the contact with leucosome.

Leucosome is medium to coarse-grained, composed of plagioclase + quartz, with sporadic large (up to 1–2 cm) hornblendes. The leucosome composition thus corresponds to tonalite and trondhjemite in contrast to metapelitic migmatites where K-feldspar is present. Mesosome is medium-grained and is composed mostly of hornblende + plagioclase + quartz ± biotite. The texture is mostly stromatitic. Tonalitic-trondhjemitic leucosome forms an anastomosing network of chaotic veins or it is interlayered with mafic mesosome. The distribution of leucosome is clearly related to deformation with quartzo-feldspathic material focused into the shear-bands, boudin necks and dilational fractures.

Within the mafic migmatites, more homogeneous bodies and lenses containing garnet and/or clinopyroxene can be observed. Massive garnet-clinopyroxene amphibolites were described by Hovorka et al. (1992) who suggested their eclogitic origin. In these rocks, the garnets rimmed by plagioclase and fine-grained clinopyroxenes, symplectitically intergrown with plagioclase, are replaced by amphiboles (Fig. 4e).

The mineral compositions of garnet-clinopyroxene amphibolites with signs of eclogite breakdown were investigated in detail:

Garnet forms subhedral grains, up to 5–10 mm in diameter, surrounded and partly resorbed by plagioclase and plagioclase-amphibole kelyphitic rims (Fig. 4e). The inclusions in the garnet cores are quartz, amphibole and rutile/ilmenite. The garnets correspond to almandine with significant grossular and pyrope contents (Table 1). Their compositions show increasing pyrope and decreasing spessartine contents as well as Fe/(Fe+Mg) ratio in rims relative to cores. Only very close to the edges, the compositional patterns become reverse, reflecting retrograde resorption and diffusion during the garnet breakdown and kelyphite formation.

Clinopyroxene forms fine-grained, glomeroblastic and vermicular grains, symplectitically intergrown with plagioclase and amphibole (Fig. 4e,f). This indicates breakdown of an older, primary clinopyroxene (Cpx I-omphacite?) to secondary clinopyroxene (Cpx II) and plagioclase. However, the characteristic "fingerprint" textures have mostly been recrystallized to granoblastic aggregates (Joanny et al. 1991). According to composition, clinopyroxene II is diopside (Table 4) with very low Al and Na contents.

Amphibole occurs as several compositional and textural types (Table 5). Amphibole I forms blue-green, small euhedral crystals enclosed in the garnet cores. Amphibole II can be recognized in kelyphitic rims around garnets as blue-green, lath-shaped crystals touching the garnet. Matrix amphiboles (Am III), at a distance from the garnet contacts, are either large, strongly pleochroic, dark-green to brown-green poikiloblastic grains, or smaller grains that replace or form part of symplectites with clinopyroxene and plagioclase (Fig. 4). These amphiboles are rather inhomogeneous (Fig. 8): close to

Table 3: Chemical compositions of biotite.

garnet-sillimanite gneisses				
	MF14/94		**MF13**	
	bt 12	**bt 7**	**bt 7**	**bt 11**
	next to grt	matrix	next to grt	matrix
SiO_2	34.91	35.75	32.43	35.77
Al_2O_3	17.84	18.8	20.17	20.34
TiO_2	3.46	3.67	0.69	1.50
MgO	13.07	12.35	12.97	13.10
FeO	15.09	14.59	18.4	14.83
MnO	0.05	0.00	0.31	0.27
CaO	0.02	0.00	0.01	0.01
Na_2O	0.06	0.11	0.08	0.28
K_2O	9.18	10.23	8.33	9.31
Σ	93.68	95.51	93.39	95.41
	Recalculated on the basis of 22 oxygens			
Si	5.310	5.332	5.027	5.312
Al^{IV}	2.690	2.668	2.973	2.688
Al^{VI}	0.509	0.638	0.707	0.872
Ti	0.396	0.412	0.080	0.167
Mg	2.963	2.745	2.993	2.899
Fe^{2+}	1.919	1.820	2.382	1.841
Mn	0.006	0.000	0.041	0.033
Ca	0.003	0.000	0.000	0.001
Na	0.018	0.032	0.024	0.080
K	1.781	1.947	1.644	1.763
$Fe^{2+}/Fe^{2+}+Mg$	0.393	0.399	0.443	0.388

Table 4: Chemical compositions of clinopyroxene.

garnet-clinopyroxene amphibolite						
			MF 16			
cpx 24	**cpx 25**	**cpx 28**	**cpx 29**	**cpx 30**	**cpx 37**
in symplectites					
53.31	53.89	53.09	53.27	53.55	53.98
1.28	1.13	1.19	0.99	0.99	1.27
0.00	0.00	0.00	0.04	0.00	0.07
10.86	11.01	11.91	11.90	12.48	11.84
11.20	10.73	11.05	10.76	10.17	10.95
0.25	0.28	0.25	0.25	0.19	0.28
21.72	22.53	21.10	21.66	21.02	20.88
0.41	0.34	0.38	0.31	0.37	0.50
0.00	0.00	0.02	0.00	0.02	0.00
99.03	99.91	98.99	99.18	98.79	99.77
Recalculated on the basis of 6 oxygens					
2.020	2.023	2.010	2.013	2.021	2.022
0.057	0.050	0.053	0.044	0.044	0.056
-	-	-	-	-	-
0.000	0.000	0.000	0.001	0.000	0.002
0.614	0.616	0.672	0.670	0.702	0.661
0.355	0.337	0.350	0.340	0.321	0.343
0.008	0.009	0.008	0.008	0.006	0.009
0.882	0.906	0.856	0.877	0.850	0.838
0.030	0.025	0.028	0.023	0.027	0.036
0.000	0.000	0.001	0.000	0.001	0.000
0.367	0.353	0.342	0.337	0.314	0.342

the garnets they are more aluminous (tschermakite) than in the matrix. Actinolite (Am IV) is a later phase that grew along fractures within earlier amphiboles.

Plagioclase compositions depend on their textural position. The plagioclase in kelyphitic rims around garnets is An_{35-38}, while in Pl-Cpx symplectites it is An_{33-34} (Table 2). The textures of plagioclase suggest that it is a secondary phase formed by the breakdown of garnet and clinopyroxene.

The *minor minerals* are mainly quartz which occurs in garnet, in kelyphites, and in the matrix. Rutile and ilmenite are ubiquitous as inclusions in garnet, matrix amphibole, and kelyphites. Sphene is abundant in the most retrograded domains and epidote-clinozoisite, biotite, chlorite and calcite have been recognized as additional retrograde minerals mostly contained in veinlets along cracks.

Geothermobarometry

Methods

Thermobarometric calculations were restricted to microtextural domains where local equilibrium between coexisting mineral phases have been assumed. Both the "conventional" and "internally consistent" thermobarometric techniques using the TWEEQU method (Berman 1991) with the thermodynamic dataset (Berman 1988) and computer program version TWQ of January 1992 were applied.

In metapelites, temperatures were calculated using several calibrations of the garnet-biotite geothermometer, i.e. Ferry & Spear (1978), Hodges & Spear (1982) Perchuk & Lavrentieva (1983), Ganguly & Saxena (1984) and Indares & Martignole (1985). Pressures were evaluated on the basis of the garnet-plagioclase-sillimanite-quartz geobarometer (GASP) using the calibrations of Newton & Haselton (1981), Hodges & Spear (1982), Ganguly & Saxena (1984), Hodges & Crowley (1985) and Koziol & Newton (1988). In the TWQ calculations, the mixing models of Berman (1990) for garnet (involving the effect of Mn), of McMullin et al. (1991) for biotite (incorporating corrections for the effect of Al and Ti) and of Fuhrman & Lindsley (1988) for feldspars were utilized along with the database.

In metabasites, temperatures were estimated by the garnet-amphibole (Graham & Powell 1984) and garnet-clinopyroxene (Ellis & Green 1979; Powell 1985) geothermometers. Pressures were calculated through the application of several geobarometers determined by suitable mineral assemblage. In those involving garnet-amphibole -plagioclase-quartz, calibrations of Kohn & Spear (1989, 1990) with both Fe- and Mg- end member reactions were used. In garnet-clinopyroxene-plagioclase-quartz assemblages, pressures were calculated from Mg- end members (GADS) according to Newton & Perkins (1982), Moecher et al. (1988), and Powell & Holland (1988). In Powell and Holland's calibration, both Hodges & Spear (1982), and Ganguly & Saxena (1984) garnet mixing models were employed. In garnet-plagioclase-rutile-ilmenite assemblages, the pressure was estimated by the (GRIPS) barometer of Bohlen & Liotta (1986). In the TWQ method, ideal mixing between tschermakite end-members in amphibole

Table 5: Chemical compositions of amphibole.

garnet-clinopyroxene amphibolite										
					MF 16					
	amp 16	**amp 5**	**amp 9**	**amp 19**	**amp 27**	**amp 36**	**amp 31**	**amp 32**	**amp 33**	**amp 35**
type	I	II	II	II	III	III	IV	IV	IV	IV
SiO_2	38.83	41.62	43.22	43.77	45.20	46.28	53.70	51.76	52.84	53.90
Al_2O_3	15.70	12.63	12.57	12.13	10.23	10.25	3.69	5.21	4.69	3.41
TiO_2	2.00	1.21	1.57	1.30	1.30	1.08	0.30	0.38	0.33	0.17
MgO	7.73	9.04	9.47	8.82	9.16	10.70	14.76	13.68	13.94	14.75
FeO	18.76	17.43	17.23	17.59	16.99	16.28	13.41	14.34	13.96	14.36
MnO	0.13	0.19	0.24	0.19	0.18	0.12	0.16	0.14	0.13	0.16
CaO	11.04	11.09	10.76	11.70	11.22	10.77	11.45	11.22	11.67	11.16
Na_2O	1.91	1.67	1.74	1.85	1.53	1.58	0.50	0.72	0.54	0.53
K_2O	1.23	0.71	0.91	0.83	0.86	0.81	0.21	0.31	0.28	0.17
Σ	97.33	95.59	97.71	98.18	96.67	97.87	98.18	97.76	98.38	98.61
Recalculated on the basis of 13 cations							15	15	15	15
Si	5.859	6.318	6.389	6.536	6.812	6.772	7.682	7.458	7.568	7.687
Al^{IV}	2.141	1.682	1.611	1.464	1.188	1.228	0.318	0.542	0.432	0.313
Al^{VI}	0.652	0.578	0.58	0.671	0.630	0.541	0.304	0.343	0.360	0.261
Ti	0.227	0.138	0.175	0.146	0.147	0.119	0.032	0.041	0.036	0.018
Fe^{3+}	0.672	0.591	0.603	0.064	0.028	0.473	0.051	0.261	0.099	0.131
Mg	1.738	2.045	2.086	1.962	2.058	2.334	3.147	2.938	2.975	3.136
Fe^{2+}	1.695	1.622	1.527	2.133	2.114	1.519	1.553	1.467	1.573	1.582
Mn	0.017	0.025	0.030	0.024	0.023	0.015	0.019	0.017	0.016	0.019
Ca	1.785	1.804	1.704	1.872	1.812	1.688	1.755	1.732	1.791	1.706
Na (M4)	0.215	0.196	0.296	0.128	0.188	0.312	0.139	0.201	0.150	0.147
Na (A)	0.343	0.295	0.203	0.408	0.259	0.137	0.000	0.000	0.000	0.000
K	0.236	0.137	0.172	0.158	0.165	0.151	0.038	0.057	0.051	0.031
Fe^{2+}/Fe^{2+}+Mg	0.494	0.442	0.423	0.521	0.507	0.394	0.330	0.333	0.346	0.335

was assumed, as well as that between diopside and hedenbergite in clinopyroxene.

Results

The metamorphic P-T conditions of metapelites were estimated in two representative samples MF 14/95 and MF 13/93.

Sample MF 14/95 (Fig. 6, Table 6) contains mineral assemblage: Grt + Sil + Bt + Pl + Kfs + Qtz. The garnet is homogenous except for a very narrow retrograde rim which is in contact with biotite. Therefore, presumed peak conditions were calculated from the composition of the garnet core, and those of biotite and plagioclase in the matrix. The temperature and pressure range is 692–850 °C and 4.5–9.8 kbar on the basis of conventional thermobarometry, and 724 ± 35 °C and 6018 ± 559 bar according to the TWQ method. Retrograde conditions were estimated from the composition in the garnet rim and those of biotite and plagioclase in contact with garnet. Temperature and pressure calculations yield 595–571 °C and 2.9–5 kbar (conventional methods) and 608 ± 29 °C at 3293 ± 1456 bar (TWQ method) respectively.

In contrast, sample MF 13/93 (Fig. 7, Table 6) contains muscovite but K-feldspar is lacking, hence the mineral assemblage is Grt + Sil + Bt + Pl + Mu + Qtz. The garnet is affected by retrograde diffusion and resorption (Fig. 5). The inferred peak conditions were obtained from the garnet core and from the composition of plagioclase inclusion in the garnet and biotite in the matrix. The temperatures and pressures calculated by conventional thermobarometry reached 615–690 °C and 4.4–7.7 kbar, the TWQ method yields 662 ± 2 °C and 6133 ± 30 bar. Retrograde conditions, estimated from the garnet rim, the biotite contacting the garnet and plagioclase near the garnet correspond to 590–635 °C and 3.7–6.4 kbar (conventional methods), as well as 615 ± 14 °C and 4495 ± 175 bar (TWQ method).

In metabasites, P-T conditions were estimated from the garnet-clinopyroxene amphibolite sample MF 16/94 (Fig. 8, Table 6). The texture shows the breakdown of garnet to plagioclase and amphibole (Amp II), which have replaced the garnet, and now form the kelyphitic rim. Moreover, the symplectite of Cpx + Pl is thought to be the breakdown product of former omphacite. Therefore, only inclusions of amphibole (Am I) enclosed in the garnet may be considered to record the prograde metamorphism, i.e. 663–692 °C (Table 6), assuming that amphibole was entrapped during the garnet growth in amphibolite facies conditions. The eclogite stage can be only inferred from reaction textures, indicating the breakdown of eclogite assemblage (garnet + Cpx I-omphacite?) to a high-pressure granulite (Grt + Cpx II + Pl + Amp II) and amphibolite assemblage (Amp III + Pl ± Grt), as observed in strongly retrograded eclogites (e.g. O'Brien 1993). Therefore, peak-pressure conditions cannot be estimated, but only those of a lower-pressure reequilibration. The compositions of garnet rim and those of kelyphitic plagioclase and amphibole (Amp II) as well as symplectitic clinopyroxene were used in several geothermometers and barometers described above. In addi-

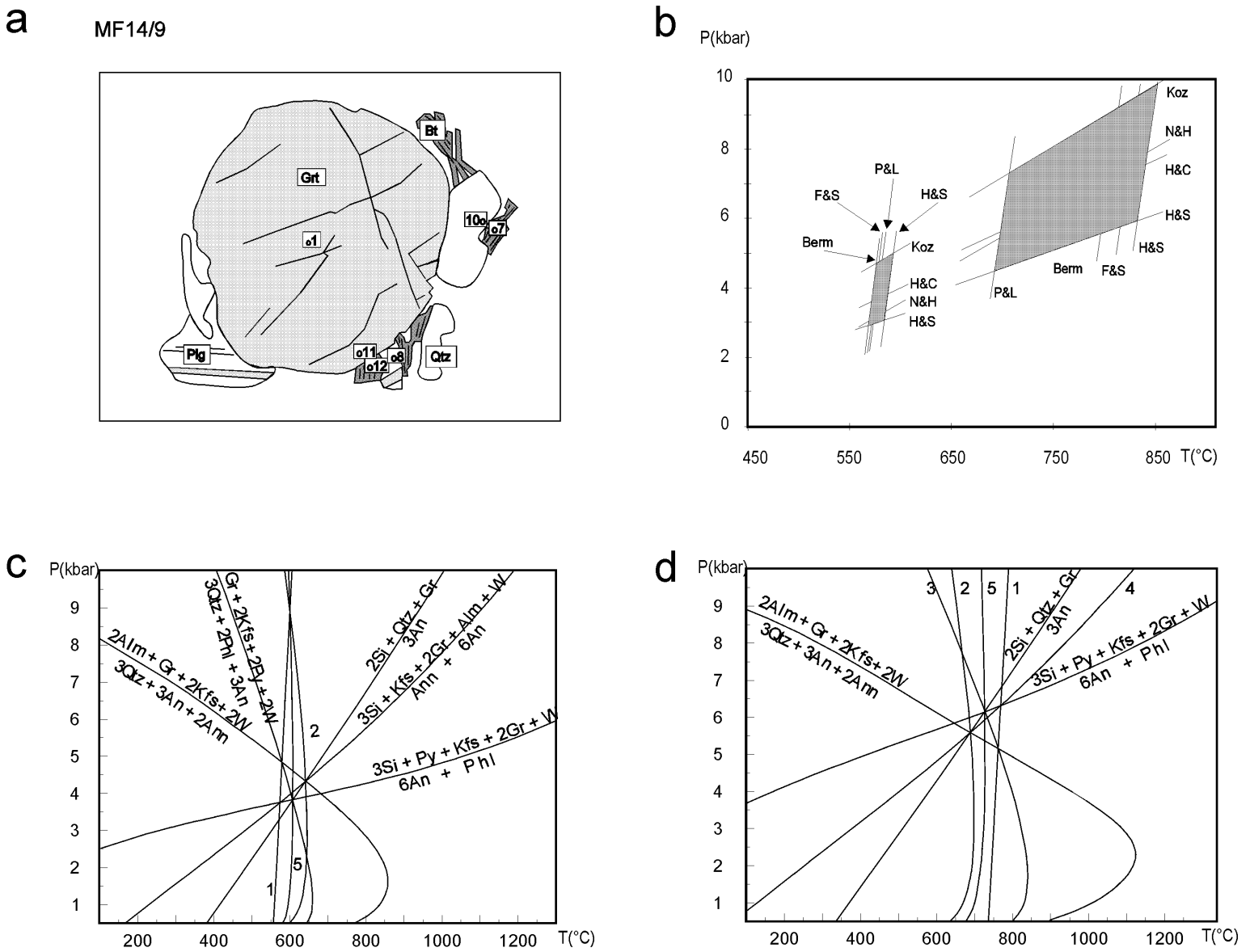

Fig. 6. Plots of thermobarometric caculations in metapelite, sample MF 14/9. **a** — Sketch of analysed points, **b** — conventional thermobarometry results, **Koz** — Koziol & Newton (1988), **N&H** — Newton & Haselton (1981), **H&C** — Hodges & Crowley (1985), **H&S** — Hodges & Spear (1982), **F&S** — Ferry & Spear (1978), **P&L** — Perchuk & Lavrentieva (1983), **Berm** — Berman (1990), **c** — WQ intersections of retrograde conditions, **d** — TWQ intersections of peak conditions. Unlabelled reactions: **1** — Phl+Alm = Ann+Py, **2** — Kfs+Alm+W = Ann+2Qtz+Si, **3** — Gr+2Kfs+2Py+2W = 3Qtz+2Phl+3An, **4** — 3Si+Kfs+2Gr+Alm+W = Ann+6An, **5** — Kfs+Py+W = Si+2Qtz+Phl.

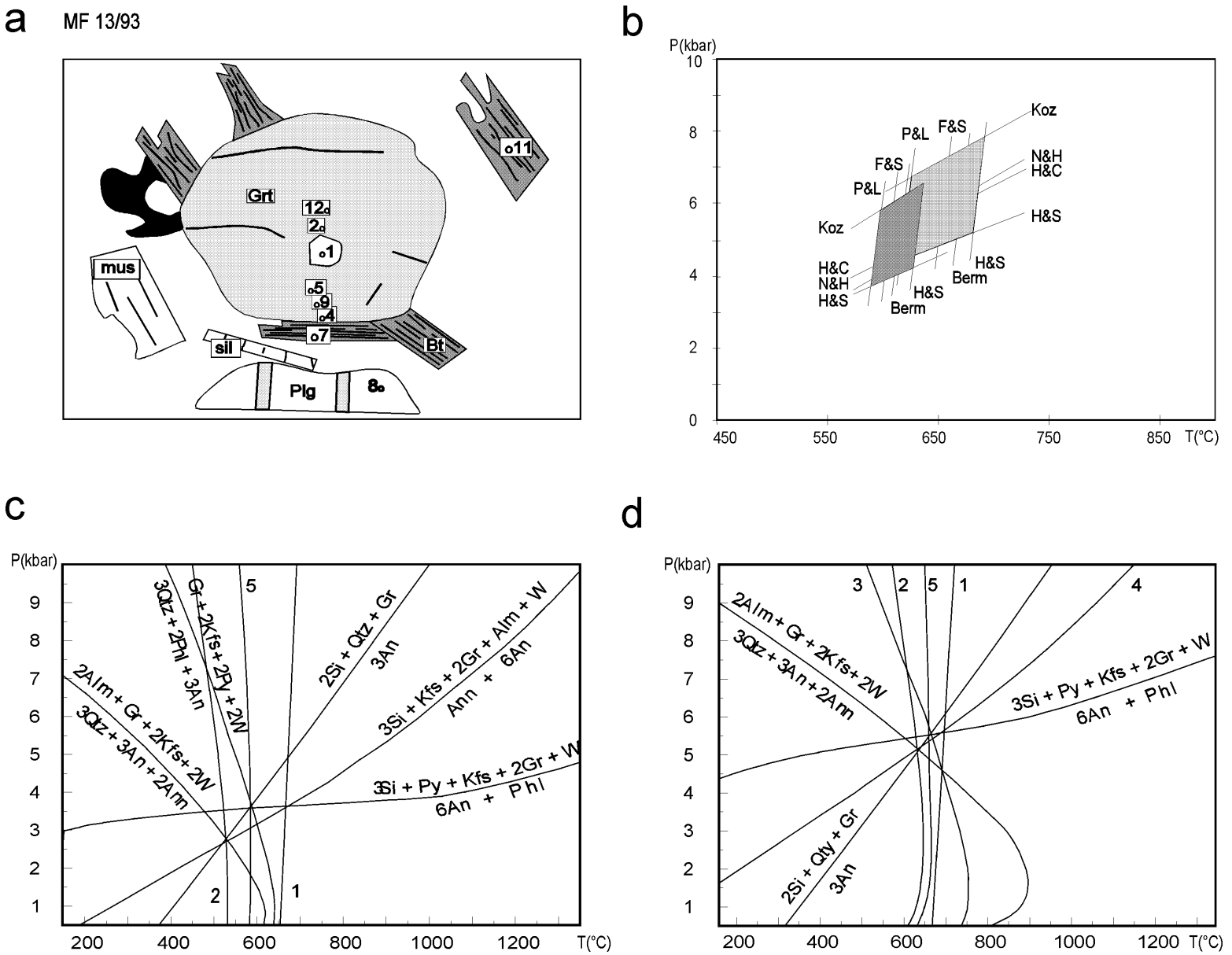

Fig. 7. Plots of thermobarometric results in metapelite, sample MF 13/93. **a** — sketch of analysed points, **b** — conventional thermobarometry results, **c** — TWQ intersections of retrograde conditions, **d** — TWQ intersections of peak conditions. Unlabelled reactions have the same numbers as in the Fig. 6.

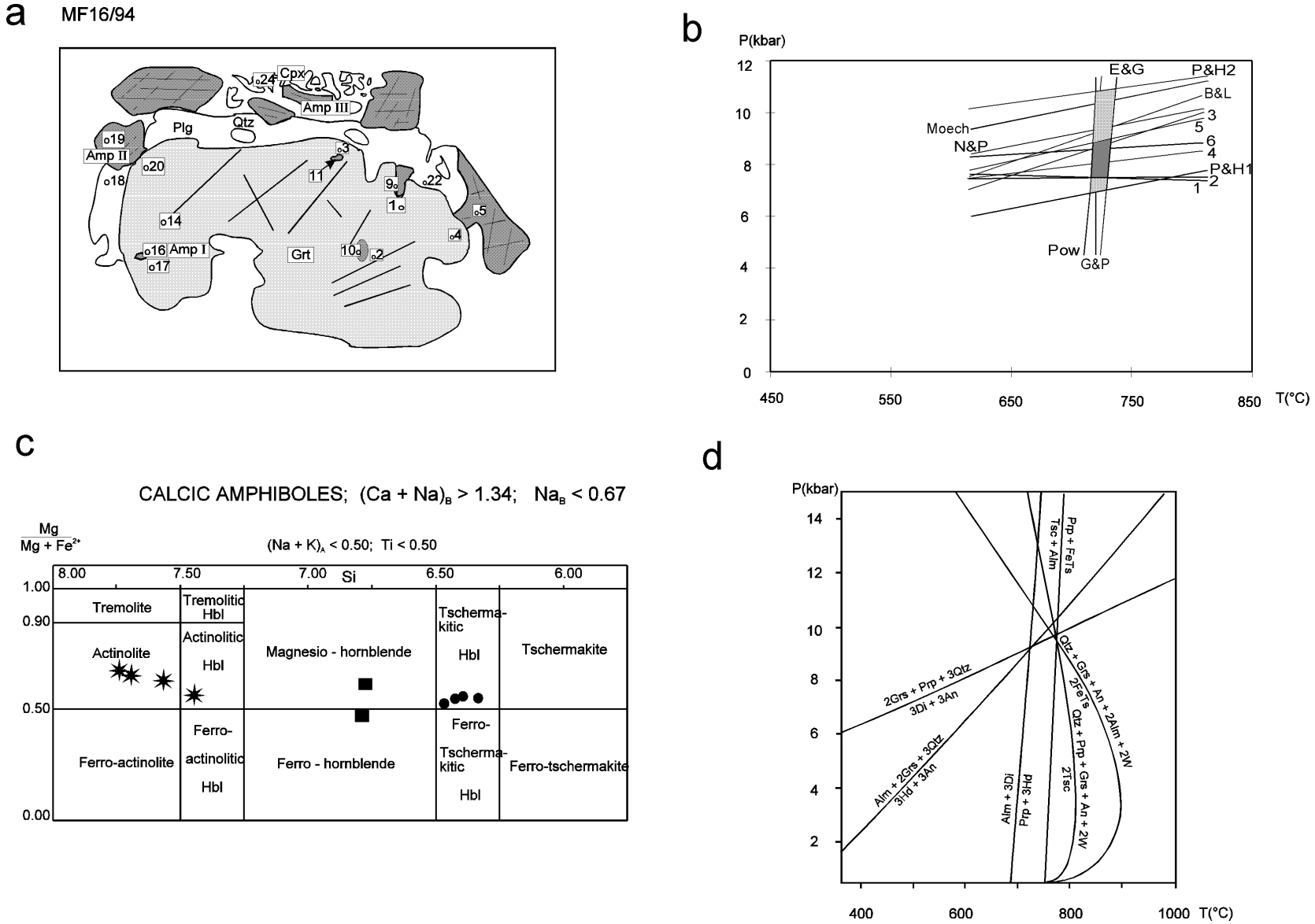

Fig. 8. Plots of thermobarometric results in garnet-clinopyroxene metabasite, sample MF 16/94. **a** — sketch of analysed points, **b** — conventional thermobarometry results of breakdown conditions, **E&G** — Ellis & Green 1983, **G&P** — Graham & Powell 1984, **Pow** — Powell 1985, **P&H** — Powell & Holland 1986, **B&L** — Bohlen & Liotta 1986, **N&P** — Newton & Perkins 1982, **Moech** — Moecher 1988, **1–6** Kohn & Spear 1989, 1990, **c** — plots of analysed amphiboles in the diagram of Leake (1978) showing Amp I and II by circles, Amp III by squares and Amp IV by stars, **d** — TWQ intersections of peak conditions.

Table 6: Summary of thermobarometric data.

Metapelites				
Sample	MF 13/93		MF 14/94	
metamorphic stage	peak	retrograde	peak	retrograde
Anal. points	grt2-bt11-plg1	grt4-bt7-plg8	grt1-bt7-plg10	grt11-bt12-plg8
Conventional thermobarometry				
T_{max} (˚C)	690 (H&S*)	635 (H&S)	850 (H&S)	595 (H&S)
P_{max} (kbar)	7.7 (Koz)	6.4 (Koz)	9.8 (Koz)	5.0 (Koz)
T_{min} (˚C)	615 (P&L)	590 (P&L)	692 (P&L)	571 (P&L)
P_{min} (kbar)	4.4 (H&S)	3.7 (H&S)	4.5 (H&S)	2.9 (H&S)
TWQ (Berman 1991)				
T (˚C)	661 (±2.5˚C)	615 (±14˚C)	724 (±35˚C)	608 (±29˚C)
P (bar)	6133 (30 bar)	4495 (±175 bar)	6018 (±559 bar)	3293 (±1456 bar)

Metabasite					
Sample MF 16					
	prograde conditions		breakdown conditions		
Anal. points	grt17-amp16	grt3-amp11	grt4-amp5	grt20-amp19	
T(˚C)	663 (G&P)	692 (G&P)	679 (G&P)	688 (G&P)	
Anal. points				grt20-cpx24	
T(˚C)	–	–	–	730-740 (E&G)	
T(˚C)	–	–	–	714-724 (Powell 1985)	
Anal. points			grt20-amp19-plg18		
P_{min} (kbar)	–	–	7.4 (Kohn & Spear 1990)		
P_{max} (kbar)	–	–	9.1 (Kohn & Spear 1990)		
Anal. points			grt20-cpx24-plg18		
P_{min} (kbar)	–	–	10.2 (Moech)	9.2 (N&P)	6.8 (P&H)
P_{max} (kbar)	–	–	10.6 (Moech)	9.4 (N&P)	10.9 (P&H)
Anal. points			grt20-ilm (ideal)-Plg18		
P_{min} (kbar)	–	–	9.1 (B&L)		
P_{max} (kbar)	–	–	9.5 (B&L)		
TWQ (Berman 1991)					
Anal. points			grt20-amp19-plg18	grt20-cpx24-plg18	
T (˚C)	–	–	768 (±0.01˚C)	716 (±0.1˚C)	
P (bar)	–	–	9656 (±0.51 bar)	9270 (±0.82 bar)	

*__Abbreviations:__ H&S — Hodges & Spear (1982), Koz — Koziol & Newton (1988), P&L — Perchuk & Lavrentieva (1983), Moech — Moecher et al. (1988), N&P — Newton & Perkins (1982), G&P — Graham & Powell (1984), E&G — Ellis & Green (1979), P&H — Powell & Holland (1986), B&L — Bohlen & Liotta (1986)

tion, the presence of rutile and ilmenite in kelyphitic domains was utilized for geobarometry.

The estimated breakdown conditions correspond to 679–740 °C and 7.4–10.9 kbar according to conventional thermobarometry (Fig. 8, Table 6). The TWQ results yield 716 °C and 9270 bar for Grt + Cpx II + Pl assemblage whereas that involving Grt + Amp II(tsch) + Pl yield 768 °C and 9656 bar which is somewhat higher even for reduced water activity in the fluid ($aH_2O = 0.7$) as shown in Fig. 8.

Discussion

The rock textures and thermobarometric data support an anatectic origin of both metapelitic and mafic migmatites ahigh-grade conditions exceeding 700 °C. Taking into consideration that diffusion has homogenized the compositions of garnet cores, peak temperatures, however, could have been even higher than obtained by geothermometry (e.g. Spear 1991; Spear & Florence 1992).

Estimated P-T conditions for metapelites are above the water saturated granite solidus (Fig. 9), thus supporting the anatectic origin of metapelitic migmatites. Moreover, as demonstrated by sample MF 14/94, muscovite-free and K-feldspar-bearing assemblages exceeded even the conditions of muscovite dehydration-melting according to Thompson (1990). Dehydration-melting of biotite (e.g. Le Breton & Thompson 1988) would require a higher temperature (ca. 750–800 °C) than indicated by thermometry, however, as discussed above, the peak temperatures are mostly obscured due to diffusion and retrogression.

The inferred kyanite-sillimanite transformation may indicate a pressure decrease at increasing temperature during "clockwise" P-T-t paths from the kyanite to the sillimanite stability field (Fig. 9). Therefore, the partial melting could have been facilitated by decompression; the crossing of the dehydration-melting curve of muscovite with positive dP/dT during the uplift is effective for increasing the volume of melt (Clemens & Vielzeuf 1987; Thompson 1990).

In metabasites, partial melting produced tonalitic to trondhjemitic leucosome, similar to field and experimental observations (e.g. Percival 1983; Hartel & Pattison 1996; Beard & Lofgren 1991; Rapp et al. 1991; Rapp & Watson 1995; Rushmer 1991; Wyllie & Wolf 1993). The P-T conditions estimated from the garnet-clinopyroxene amphibolite are above the water-

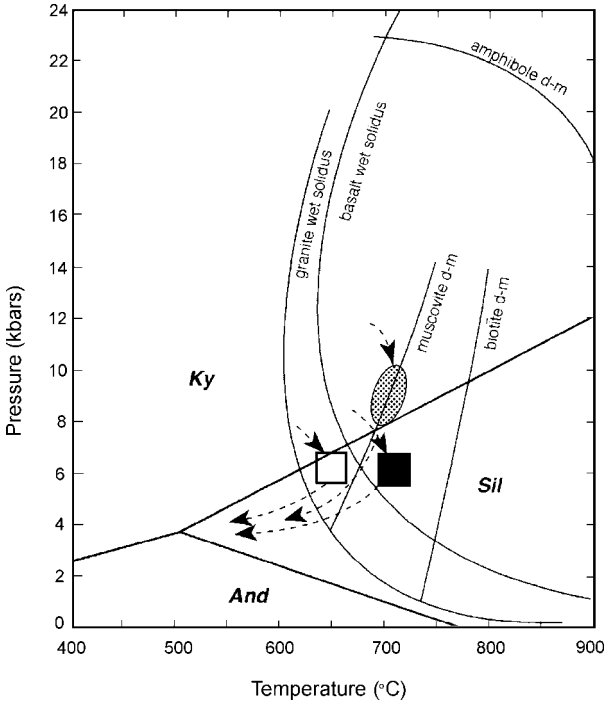

Fig. 9. Pressure-temperature diagram showing tentative P-T paths of analysed samples with respect to melting conditions. *Shaded ellipse:* Grt — Cpx metabasite (MF 16/94), *black square:* Kfs — bearing and Mu — free metapelite (MF 14/94), *white square:* Mu — bearing and Kfs — free metapelite (MF 13/93). Melting equilibria are from Thompson (1990 and references therein) and Wyllie & Wolf (1993). Alumosilicate stabilities are according to Holdaway (1971).

saturated solidus of basalt (Fig. 9), hence partial melting as a major process of migmatitization is possible. The calculated temperatures are below most experimentally investigated amphibole dehydration-melting equilibria in fluid absent conditions (see references above). However, as pointed out by Wyllie & Wolf (1993), the amphibolite dehydration-melting solidus and the melting interval for a fully-hydrated amphibolite (hornblende + plagioclase) producing liquid and garnet-amphibolite residues can be largely expanded to much lower temperatures and pressures than the other experimental results.

As indicated by reaction textures, the Malá Fatra metabasites most probably followed the "clockwise" P-T-t trajectories (Fig. 9) from higher-pressure (eclogite facies) conditions. They were reequilibrated, and most probably also melted, at conditions which are transitional between the amphibolite and high-pressure granulite facies (e.g. Bucher & Frey 1994). This is indicated by the assemblage Grt + Cpx + Plg + Qtz in the breakdown domains. The absence of orthopyroxene indicates that conditions of high-temperature, medium-pressure granulite facies were not reached. Alternatively, orthopyroxene could have been totally consumed by amphibole due to "rehydration-crystallization" of the trondhjemite melt during the retrograde portion of the P-T-t path (e.g. Stevens & Clemens 1993; Brown 1994).

Taking into consideration the above reconstructed P-T-t paths, decompressional, dehydration-melting in both- metapelite and metabasite protoliths could be a viable process of migmatitization in the Malá Fatra crystalline basement.

The estimated P-T conditions indicate that melting took place at deep-crustal levels corresponding to 5–10 kbar, whereas the emplacement of granitoids in the northern part of the Malá Fatra, estimated from the amphibole barometry (Benko 1996; Broska et al. 1997) corresponds to 3–3.5 kbar. The textures observed in the migmatites suggest close relationships between melt distribution and deformation, hence the melt could have been extracted from its source and transported via a network of shear zones and fractures structurally upwards, forming more voluminous portions of the melt collecting into the pluton (e.g. Hollister & Crawford 1986; Clemens & Mawer 1993; Collins & Sawyer 1996). Field relations and the geological structure in the profile across the southern part of the Malá Fatra (Fig. 2) demonstrate that there is an increasing abundance of melt structurally upwards, i.e. from migmatitic gneisses and amphibolites to the "hybrid" granitoids (granodiorites and tonalites).

The Malá Fatra crystalline basement closely resembles the situation in some other areas in the Central Western Carpathians (mainly the Tatra Mts. and Low Tatra Mts.), where high-grade metamorphism and partial melting of lower-crustal protoliths has been documented (Janák et al. 1988, 1995, 1996; Janák 1994; Krist et al. 1992; Hovorka et al. 1993; Petrík et al. 1994). Generally south to southeast-vergent, syn- to post-metamorphic penetrative deformation, decompression from high-pressure (eclogite facies) and recrystallization at medium-pressure and high-temperature conditions accompanied by partial melting is characteristic for the Variscan tectono-metamorphic evolution of the Western Carpathian basement, similar to the situation in the Central European Variscides (e.g. Matte 1986; Neubauer & Von Raumer 1993).

Acknowledgements: This paper is part of the MSc thesis of B.L., supported by Department of Mineralogy and Petrology, Comenius University Bratislava. We are grateful to Pavol Siman (Geological Survey, Bratislava) for the help with the microprobe analyses. Milan Kohút (Geological Survey, Bratislava), Pavel Pitoňák (Geol. Inst. Academy of Science, Banská Bystrica) and Lívia Ludhová (Comenius University, Bratislava) are thanked for their help during the field work. Peter Nábělek (University of Missouri, Columbia) and Ján Spišiak (Geol. Inst. Academy of Science, Banská Bystrica) provided very helpful and constructive reviews, which greatly improved the manuscript.

References

Ashworth J. R., 1985: Introduction. In: Ashworth J.R. (Ed.): *Migmatites. Blackie,* Glasgow, 1–35.

Beard J.S. & Lofgren G.E., 1991: Dehydration melting and water-saturated melting of basaltic and andesitic greenstones and amphibolites at 1, 3, and 6.9 kbar. *J. Petrology,* 32, 365–401.

Benko P., 1996: Geochemical and mineralogical study of granitoid rocks in the Kriváň massif of the Malá Fatra Mts. *M.Sc.thesis, Department of Mineralogy and Petrology, Comenius University,* Bratislava, 1–80.

Berman R.G., 1990: Mixing properties of Ca-Mg-Fe-Mn garnets. *Amer. Mineralogist,* 75, 328–344.

Berman R.G., 1991: Thermobarometry using multi-equilibrium calculations: a new technique, with petrological applications. *Canad. Mineralogist*, 29, 833–855.

Bohlen S.R. & Liotta J.J., 1986: A barometer for garnet amphibolites and garnet granulites. *J. Petrology,* 27, 1025–56.

Broska I., Petrík I. & Benko P., 1997: Petrology of the Malá Fatra granitoid rocks (Western Carpathians, Slovakia). *Geol. Carpathica,* 48, 1, 27–37.

Brown M., 1994: The generation, segregation, ascent and emplacement of granite magma: the migmatite-to-crustally-derived granite connection in thickened orogens. *Earth Sci. Rev.,* 36, 83–130.

Bucher K. & Frey M., 1994: Petrogenesis of Metamorphic rocks. *Springer-Verlag,* 1–318.

Clemens J.D. & Mawer C.K., 1992: Granite magma transport by fracture propagation. *Tectonophysics,* 204, 339–360.

Clemens J.D. & Vielzeuf D., 1987: Constraints on melting and magma production in the crust. *Earth Planet. Sci. Lett.,* 86, 287–306.

Collins W.J. & Sawyer E.W., 1996: Pervasive granitoid magma transfer through the lower-middle crust during non-coaxial compressional deformation. *J. Metamorphic Geol.,* 14, 565–579.

Ellis D.J. & Green D.H., 1979: An experimental study of the effect of Ca upon garnet-clinopyroxene Fe-Mg exchange equilibria. *Contr. Mineral. Petrology*, 71, 13–22.

Fuhrman M. & Lindsley D., 1988: Ternary - feldspar modelling and thermometry. *Amer. Mineralogist*, 73, 201–215.

Ganguly J. & Saxena S.K., 1984: Mixing properties of aluminosilicate garnets: constraints from natural and experimental data and applications to geothermo-barometry. *Amer. Mineralogist*, 69, 88–97.

Graham C.M. & Powell R., 1984: A garnet-hornblende geothermometer and application to the Pelona schists, southern California. *J. Metamorphic Geol.,* 2, 13–22.

Hartel T.H.D & Pattison D.R.M., 1996: Genesis of the Kapuskasing (Ontario) migmatitic mafic granulites by dehydration melting of amphibolite: the importance of quartz to reaction progress. *J. Metamorphic Geol.,* 14, 591–611.

Hodges K.V. & Spear F.S., 1982: Geothermometry, geobarometry and the Al_2SiO_5 triplepoint at Mt. Moosilauke, New Hampshire. *Amer. Mineralogist*, 67, 1118–1134.

Hodges K.V. & Crowley, 1985: Error estimation for empirical geothermometry for pelitic system. *Amer. Mineralogist*, 70, 702–709.

Holdaway M.J., 1971: Stability of andalusite and the aluminium silicate phase diagram. *Amer. J. Sci.,* 271, 97–245.

Hollister L.S., 1966: Garnet zoning: an interpretation based on the Rayleigh fractionation model. *Science,* 154, 1647–1651.

Hollister L.S. & Crawford M.L., 1986: Melt-enhanced deformation: a major tectonic process. *Geology,* 14, 558–561.

Hovorka D., 1967: Porphyrites and lamprophyres of the tatroveporic crystalline. *Sbor. Geol. Vied, Západ. Karpaty,* 8, 51–78.

Hovorka D., 1969: Metasomatic alterations of amphibolites in the Malá Fatra. *Geol. Práce, Spr.,* 49, 5–61.

Hovorka D., 1974: Amphibolites of migmatite areas, West Carpathian Mts. *Chemie der Erde,* 33, 3, 221–242.

Hovorka D., Ivan P., Kratochvíl M., Reichwalder P., Rojkovič I., Spišiak J. & Turanová L., 1985: Ultramafic rocks of the Western Carpathians. *GÚDŠ,* Bratislava, 1–258.

Hovorka D. & Méres Š., 1991: Pre-upper carboniferous gneisses of the Strážovské Vrchy upland and the Malá Fatra Mts. *Acta geol. geogr. Univ. Comen., Geol*., 46, 103–70.

Hovorka D., Méres Š. & Caňo F., 1992: Petrology of the garnet-clinopyroxene metabasites from the Malá Fatra Mts. *Miner. slovaca*, 24, 45–52.

Hovorka D., Méres Š. & Ivan P., 1994: Pre-Alpine Western Carpathians basement complexes: lithology and geodynamic setting. *Mitt. Österr. Geol. Gesell.,* 86, 33–44.

Indares A. & Martignole J., 1985: Biotite-garnet geothermometry in granulite facies: influence of Ti and Al in biotite. *Amer. Mineralogist*, 70, 272–278.

Ivanov M. & Kamenický L., 1957: Contributions to geology and petrology of the Malá Fatra crystalline. *Geol. Práce, Zoš.*, 45, 180–216.

Janák M., 1994: Variscan uplift of the crystalline basement, Tatra Mts., Central Western Carpathians: Evidence from $^{40}Ar/^{39}Ar$ laser probe dating of biotite and P-T-t paths. *Geol. Carpathica*, 45, 293–300.

Janák M., Kahan S. & Jančula D., 1988: Metamorphism of pelitic rocks and metamorphism in SW part of Western Tatra Mts. crystalline complexes. *Geol. Carpathica*, 39, 455–488.

Janák M., Pitoňák P., Spišiak J., Petrík I. & O'Brien P.J., 1995: Trondhjemitic-tonalitic melts in the Western Carpathian basement: implications for partial melting of amphibolite and differentiation of the lower crust. *Terra Abstr.,* Suppl. 1, 7.

Janák M., O'Brien P.J., Hurai V. & Reutel Ch., 1996: Metamorphic evolution and fluid composition of garnet-clinopyroxene amphibolites from the Tatra Mountains, Western Carpathians. *Lithos,* 39, 57–79.

Joanny V., van Roermund H. & Lardeaux J.M., 1991: The clinopyroxene/plagioclase symplectite in retrograde eclogites: a potential geothermobarometer. *Geol. Rdsch*., 80, 303–320.

Kamenický L. & Macek J., 1984: Ein profil durch die lithostratigraphischen schichtenfolgen des kristallinikum des gebirges Malá Fatra. *Geol. Zbor. Geol. Carpath*., 35, 157–160.

Kamenický L., Macek J. & Krištín J., 1987: Contribution to petrography and geochemistry of granitoids in the Malá Fatra. *Miner. slovaca,* 19, 311–324.

Kohn M.J. & Spear F.S., 1989: Empirical calibration of geobarometers for the assemblage garnet + hornblende + plagioclase + quartz. *Amer. Mineralogist*, 74, 77–84.

Kohn M.J. & Spear F.S., 1990: Two new geobarometers for garnet amphibolites, with applications to Southeastern Vermont. *Amer. Mineralogist,* 75, 89–96.

Korikovsky S.P, Kamenický L, Macek J. & Boronikhin V.A., 1987: P-T conditions of metamorphism of the crystalline schists in the Malá Fatra (in the profile of the Mlynský Potok area). *Geol. Zbor. Geol. Carpath.,* 38, 409–427.

Koziol A.M. & Newton R.C., 1988: Redetermination of the anorthite breakdown reaction and improvement of the plagioclase-garnet-Al_2SiO_5-quartz geobarometer. *Amer. Mineralogist*, 73, 216–233.

Krist E., Korikovsky S.P., Putiš M., Janák M. & Faryad S.W., 1992: Geology and petrology of metamorphic rocks of the Western Carpathian crystalline complexes. *Comenius University Press*, Bratislava, 1–324.

Kretz R., 1983: Symbols for rock-forming minerals. *Amer. Mineralogist*, 68, 277–279.

Leake B.E., 1978: Nomenclature of amphiboles. *Amer. Mineralogist*, 63, 1023–1052.

Le Breton N. & Thompson A.B., 1988: Fluid-absent (dehydration) melting of biotite in metapelites in the early stages of crustal anatexis. *Contr. Mineral. Petrology,* 99, 226–237.

Lupták B., 1996: Petrological and petrotectonic study of metamorphic rocks in the Malá Fatra (Veľká Lúka Massif). *M.Sc. thesis. Department of Mineralogy and Petrology, Comenius university, Bratislava*, 1–81.

McMullin D.W.A., Berman R.G. & Greenwood H.J., 1991: Calibration of the SGAM thermobarometer for pelitic rocks using data from phase equilibrium experiments and natural assemblages. *Canad. Mineralogist*, 29, 889–908.

Moecher D.P., Anovitz L.M. & Essene E.J., 1988: Calculation of clinopyroxene-garnet-plagioclase-quartz geobarometers and application to high grade metamorphic rocks. *Contr. Mineral. Petrology*, 100, 92–106.

Neubauer F. & von Raumer J.F., 1993: The Alpine basement - linkage

between variscides and East-Mediterranean mountain belts. In: J. F. von Raumer & F. Neubauer (Eds.): *Pre-Mesozoic geology in the Alps. Springer-Verlag,* Berlin-Heidelberg, 641–663.

Matte P., 1986: Tectonics and plate tectonics model for the Variscan belt of Europe. *Tectonophysics,* 126, 329–374.

Newton R.C. & Haselton H.T., 1981: Thermodynamics of the garnet-plagioclase-Al_2SiO_5-quartz geobarometer. In: Newton R.C. Navrotsky A. & Wood B.J. (Eds.): *Thermodynamics of Minerals and Melts. Advances in Physical Geochemistry, Vol. 1, Springer-Verlag*, New York, 129–145.

Newton R.C. & Perkins D., 1982: Thermodynamic callibration of geobarometers based on the assemblages garnet-plagioclase-orthopyroxene (clinopyroxene)-quartz. *Amer. Mineralogist,* 67, 203–222.

O'Brien P.J., 1993: Partially retrograded eclogites of the Münchberg Massif, Germany: records of a multistage Variscan uplift history in the Bohemian Massif. *J. Metamorphic Geol.,* 11, 241–260.

Percival J.A., 1983: High-grade metamorphism in the Chapleau-Foleyet area, Ontario. *Amer. Mineralogist*, 68, 667–686.

Perchuk L.L. & Lavrentieva I.V., 1983: Experimental investigations of the exchange equilibria in the systems cordierite-garnet-biotite. In: Saxena S.K. (Ed.): *Kinetics and equilibrium in Mineral Reactions. Advances in Physical Geochemistry, Vol.3. Springer-Verlag,* New York, 199–240.

Perchuk L.L., Lavrentieva I.V., Aranovich L.J. & Petrík I., 1984: Comparative characteristics of thermodynamic regimes of metamorphic rocks from Caucasus ridge and Western Carpathians. *Geol. Zbor. Geol. Carpath.*, 37, 3, 33–363.

Petrík I., Broska I. & Uher P., 1994: Evolution of the Western Carpathians granite magmatism: Age, source rock, geotectonic setting and relation to the Variscan structure. *Geol. Carpathica*, 42, 5, 283–291.

Powell R. & Holland T.H.B., 1988: An internally consistent thermodynamic dataset with uncertainties and correlations: 3. Applications to geobarometry, worked examples and a computer program. *J. Metamorphic Geol.,* 6, 173–204.

Powell R., 1985: Regression diagnostics and robust regression in geothermometer/geobarometer calibration: the garnet-clinopyroxene geothermometer revisited. *J. Metamorphic Geol.,* 3, 327–342.

Rapp R.P., Watson E.B & Miller C.F., 1991: Partial melting of amphibolite/eclogite and the origin of Archean trondhjemites and tonalites. *Precambrian Research*, 51, 1–25.

Rapp R.P. & Watson E.B., 1995: Dehydration melting of metabasalt at 8–32 kbar: Implications for continental growth and crust-mantle recycling. *J. Petrology*, 36, 891–931.

Rushmer T., 1991: Partial melting of two amphibolites: contrasting experimental results under fluid-absent conditions. *Contr. Mineral. Petrology*, 107, 41–59.

Scherbak N.P., Cambel B., Bartnitsky E.N. & Stepanyuk L.M., 1990: U-Pb age of granitoids rock from the quarry Dubná Skala-Malá Fatra Mts. *Geol. Zbor. Geol. Carpath.,* 41, 4, 407–414.

Spear F.S., 1991: On the interpretation of peak metamorphic temperatures in light of garnet diffusion during cooling. *J. Metamorphic Geol.,* 9, 379–388.

Spear F.S. & Florence F.P., 1991: Thermobarometry in granulites: pitfalls and new approaches. *Precambrian Research*, 55, 209–241.

Stevens G. & Clemens J.D., 1993: Fluid-absent melting and the roles of fluids in the lithosphere: a slanted summary? *Chem. Geol.*, 108, 1–17.

Thompson A.B., 1990: Heat, fluids, and melting in the granulite facies. In: D.Vielzeuf & Ph.Vidal (Eds.): *Granulites and Crustal Evolution NATO. ASI Series, Vol. 311, Kluwer*, Dordrecht, 37–57.

Woodsworth G.J., 1977: Homogenisation of zoned garnet from pelitic schists. *Canad. Mineralogist,* 15, 230–242.

Wyllie P.J. & Wolf M.B., 1993: Amphibolite dehydration-melting: sorting out the solidus. In: H.M. Prichard, T. Alabaster, N.B.W. Harris & C.R. Neary (Eds.): *Magmatic processes and plate tectonics. Geological Society Special Publication*, 76, 405–416.

Yardley B.W.D., 1977: An empirical study of dffusion in garnet. *Amer. Mineralogist,* 62, 793–800.